

# RSC Advances



This is an *Accepted Manuscript*, which has been through the Royal Society of Chemistry peer review process and has been accepted for publication.

*Accepted Manuscripts* are published online shortly after acceptance, before technical editing, formatting and proof reading. Using this free service, authors can make their results available to the community, in citable form, before we publish the edited article. This *Accepted Manuscript* will be replaced by the edited, formatted and paginated article as soon as this is available.

You can find more information about *Accepted Manuscripts* in the [Information for Authors](#).

Please note that technical editing may introduce minor changes to the text and/or graphics, which may alter content. The journal's standard [Terms & Conditions](#) and the [Ethical guidelines](#) still apply. In no event shall the Royal Society of Chemistry be held responsible for any errors or omissions in this *Accepted Manuscript* or any consequences arising from the use of any information it contains.

**Plasma Modified SnO<sub>2</sub>:F Substrate for Efficient Cobalt Selenide Counter in Dye  
Sensitized Solar Cell**

Yudan Luo, Rui Cheng, Jie Shen, Xiaohong Chen, Zhe Lu, Yiwei Chen, Zhuo Sun,  
Sumei Huang\*

Engineering Research Center for Nanophotonics & Advanced Instrument, Ministry of  
Education, Department of Physics, East China Normal University, North Zhongshan  
Rd. 3663, Shanghai 200062, P. R. China

**Abstract**

Cobalt selenide (Co<sub>0.85</sub>Se) counter electrodes (CEs) were in-situ synthesized on the plasma-treated fluorine doped tin oxide (FTO) substrates using a hydrothermal approach. FTO glass substrates were treated using O<sub>2</sub>/ Ar direct current (DC) plasma for 5 min prior to the cobalt selenide growth. It was found that Co<sub>0.85</sub>Se developed horizontally and vertically oriented, submicron or micron sized, and tremelliform like structures on the plasma modified FTO surface. This unique Co<sub>0.85</sub>Se nanomaterial had a much larger accessible surface area, more active catalytic sites and better catalytic properties, compared to the case without plasma treatment. The electronic and ionic processes in dye sensitized solar cells (DSSCs) based on cobalt selenide

---

\*Corresponding author: Fax: +86 21 62234321.

E-mail address: smhuang@phy.ecnu.edu.cn (Sumei Huang).

CEs with or without plasma treatment as well as the Pt CE are analyzed and compared. The device with the  $\text{Co}_{0.85}\text{Se}$  on the plasma-treated FTO produces an energy conversion efficiency of 8.04%, which is significantly superior to that for the DSSC with the Pt CE (7.66%), and also higher than that (7.88%) for the device with the  $\text{Co}_{0.85}\text{Se}$  CE on the pristine FTO without plasma treatment. Plasma treatment of transparent conducting oxides has been proposed as an effective method for in-situ deposition of high-quality inorganic compound CE nanomaterials and improving their electrocatalytic activities of inorganic compound CEs.

**Keywords:** Cobalt selenide; plasma treatment; fluorine doped tin oxide; counter electrode; dye sensitized solar cells

## 1. Introduction

Dye sensitized solar cells (DSSCs) have been studied intensively due to their advantages in economic, scientific and technical aspects since their conversion efficiencies exceeded 11% [1-3]. The classical DSSC has a sandwich-type structure consisting of a counter electrode (CE), an electrolyte, and a dye-sensitized photoanode. The mission of a CE is the reduction of redox species used as a mediator in regenerating the sensitizer after electron injection in a liquid-state/quasi-solid state DSSC, or collection of the holes from the hole-conducting material in a solid state DSSC [1, 4]. The standard CE used in DSSCs is fluorine-doped tin oxide (FTO) glass supported platinum (Pt), which is normally prepared by a sputtering or thermal decomposition method. A FTO supported Pt CE has high conductivity, excellent electrocatalytic activity, and good chemical stability. However, the high cost of the noble metal Pt and the possible decomposition of the Pt in the  $I_3^- / I^-$  redox couple electrolyte restrain the large-scale fabrication and long-term stability of the DSSCs. Therefore, considerable efforts have been made to explore low-cost and stable alternatives to replace Pt CE. Many low-cost materials, such as conducting polymers [5], graphene [6, 7], carbon [8-10], nitrides [11, 12], sulfides [13-15] and selenides [16-18] have been successfully used for CEs. Despite numerous investigations, only a few materials have shown performance better than platinum [19]. Recently, Gong et al synthesized  $Co_{0.85}Se$  and  $Ni_{0.85}Se$  non-Pt CEs by a low-temperature hydrothermal approach [16]. The power conversion efficiency (PCE) of the DSSC based on the grown  $Co_{0.85}Se$  CE is 0.76 % higher than that of the device based on the Pt CE. The

$\text{Co}_{0.85}\text{Se}$  CE exhibited obviously higher electrocatalytic activity than Pt for the reduction of triiodide, but  $\text{Ni}_{0.85}\text{Se}$  showed inferior catalytic activity than Pt. In another work, they used  $\text{NiSe}_2$  as CE, and the DSSCs produced a PCE of 8.69%, higher than the Pt CE based DSSCs (8.04%) [20]. CoSe prepared by an electro-deposition method was employed as CEs for DSSCs. After optimization, the DSSCs gave a PCE of 7.30%, higher than the DSSCs using Pt CE (6.91%) [21]. Guo et al prepared  $\text{NbSe}_2$  nanosheets (NSs) and nanorods (NRs) via a solvothermal approach. The prepared NSs and NRs were used as CEs for DSSCs, which produced PCE values of 7.34 and 6.78%, close to Pt CE based DSSCs (7.90%) [22]. A ternary selenide  $\text{CuInGaSe}_2$  CE prepared by a magnetron sputtering technology was reported to give a PCE of 7.13% in its DSSC device, comparable to the efficiency of the DSSC using a Pt CE (6.89%) [18]. We also explored a simple, eco-friendly and screen-printing process for quaternary selenide  $\text{Cu}_2\text{ZnSn}(\text{S},\text{Se})_4$  (CZTSSe) CEs and achieved a PCE of 5.75 % [17]. The catalytic activity of selenides as CEs are affected significantly by the morphological, physical (i.e., particle size, porosity, crystal structure) and chemical properties of nanoselenides, however, none of which is adequately addressed. Moreover, the mechanism of the catalytic activity of selenides for regeneration of the electrolyte is poorly understood.

Low-temperature plasma is an effective tool for the fabrication and manipulation of nano-materials and thin films [23]. It has been previously applied for surface modification/optimization of various nano-materials and thin films, including

different transparent conducting oxides (TCOs) such as indium tin oxide (ITO) [24], zinc oxide (ZnO) [25], FTO [26] and TiO<sub>2</sub> films [27-29] with different gas combinations such as argon, hydrogen, oxygen, carbon tetrafluoride or sulfur hexafluoride. Enhancement of the DSSC performance has been demonstrated by plasma treatments of TiO<sub>2</sub> films due to the increase in surface hydrophilicity and nanoparticles packing density and improvement of oxide's stoichiometry, leading to increased dye loading as well as improved electron transport and reduced recombination [28, 29].

In this paper, we propose the use of plasma-treated FTO glass as a substrate for growth of cobalt selenide CEs for DSSCs via an in-situ deposition method. We aim to advance the understanding of the structural features of cobalt selenide CEs assisted by plasma treatment and their effect on the photovoltaic performance of the device. The FTO glass substrates were treated using 20 sccm O<sub>2</sub>/ 30 sccm Ar plasma for 5 min prior to the nano-selenide growth. Cobalt selenide (Co<sub>0.85</sub>Se) was synthesized in-situ on the plasma-treated FTO substrates using a modified hydrothermal method [16]. For comparison, cobalt selenide on the pristine FTO glass substrate was prepared using the same hydrothermal approach, and the Pt on the pristine FTO was fabricated using the thermal decomposition method. The grown cobalt selenide was applied directly as CEs to assemble DSSCs without any post-treatments. Catalytic properties of cobalt selenide nanomaterials for reduction of I<sub>3</sub><sup>-</sup> were examined by cyclic voltammetry (CV) and electrochemical impedance spectroscopy (EIS). The cell with the Co<sub>0.85</sub>Se

on the plasma-treated FTO produces an energy conversion efficiency of 8.04%, which is conspicuously higher than that for the DSSC with the Pt CE (7.66%), and also higher than that (7.88%) for the device with the CoSe CE on the pristine FTO without plasma treatment.

## 2. Experimental

### 2.1 Preparation of cobalt selenide and Pt CEs

Se powders,  $\text{CoCl}_2 \cdot 6\text{H}_2\text{O}$  and  $\text{N}_2\text{H}_4 \cdot \text{H}_2\text{O}$  were purchased from Sinopharm Chemical Reagent Co., Ltd., China. The reagents were used as received without further purification. Transparent conductive glass (F-doped  $\text{SnO}_2$ , FTO,  $15 \Omega/\text{square}$ , Nippon Sheet Glass Co., Ltd., Japan) was used as the substrate material. FTO substrates were cleaned by sonication in glass detergent (Hui Jie washing Ltd., Shenzhen), acetone and isopropyl alcohol, and subsequently dried in a vacuum oven. The cleaned FTO glass was treated using 20 sccm  $\text{O}_2$  / 30 sccm Ar plasma for 5 min prior to the selenide nanomaterial growth. The direct current (DC) plasma power was set at 30 W. The working pressure was about 40 Pa. Next, Se powders (0.048 mmol, 99.0% in purity) and  $\text{CoCl}_2 \cdot 6\text{H}_2\text{O}$  (0.04 mmol) were dissolved in 11 mL of deionized water. The resulted mixture was transferred to a 100 mL Teflon-lined autoclave. Then, 3.0 mL of  $\text{N}_2\text{H}_4 \cdot \text{H}_2\text{O}$  (85 wt %) was added in the autoclave with vigorous stirring for 10 min. The plasma-treated FTO substrates were put into the autoclave and placed at an angle against its Teflon liner wall with the substrate conducting layer facing down. The autoclave was sealed and maintained at 120 °C for 8 h, which is shorter than that

reported in ref. [16]. For comparison, cobalt selenide and Pt were prepared on the pristine FTO glass substrates without plasma treatment. The former was prepared using the same hydrothermal method described in the above. The latter was printed using a paste based on  $\text{H}_2\text{PtCl}_6$  dispersed in a mixture of terpineol and ethylcellulose. The printed layers were heated at  $385^\circ\text{C}$  for 20 min [30].

## 2.2 Fabrication of DSSCs

The  $\text{TiO}_2$  working electrodes with a total thickness of about  $16\ \mu\text{m}$  on the FTO glass plates were prepared according to the procedures described in our previous work [6]. The as-prepared photoanodes was dipped in a dye solution (0.5 mM N719 (Solaronix) in acetonitrile and tert-butyl alcohol (volume ratio of 1:1)) at room temperature for 20 h. The cells were sealed with Surlyn 1702 (Dupont) gasket with a thickness of  $60\ \mu\text{m}$ . A drop of electrolyte solution (0.05M  $\text{I}_2$ , 1M MPPII, 0.5M Guanidine Thiocyanate and 0.5M tert-butylpyridine in acetonitrile) was injected into the inter-space between the photoanode and CE. Finally, the holes on the back of the CE were sealed with a Surlyn film and covered with a thin glass slide under heat.

## 2.3 Characterization

The morphologies and microstructures of the formed inorganic compound counter-electrode layers were characterized by field emission scanning electron microscopes (FESEM, S4800, Hitachi and JSM-7001F, JEOL) and X-ray diffractometer (XRD, Rigaku ULTIMA IV, D/tex detector,  $\text{Cu-K}\alpha$ :  $\lambda = 0.15406\ \text{nm}$ ).

The thickness of the layers were measured by a profilometer (Dektak 6M). EIS and CV measurements of DSSCs were recorded with a galvanostat (PG30.FRA2, Autolab, Eco Chemie B. V Utrecht, Netherlands) under illumination  $100 \text{ mW cm}^{-2}$ . The electrolyte was the same as used in DSSCs. The frequency range was from 10 to 100 KHz, and the applied bias voltage and ac amplitude were set at open-circuit voltage and 10 mV, respectively, between the counter electrode and the working electrode. The impedance spectra were analyzed by an equivalent circuit model, interpreting the characteristics of the DSSCs [31, 32]. Photocurrent–voltage (*I-V*) measurements were performed using an AM 1.5 solar simulator equipped with a 1000W Xenon lamp (Model No. 91192, Oriel, USA). The solar simulator was calibrated by using a standard Silicon cell (Newport, USA). The light intensity was  $100 \text{ mW cm}^{-2}$  on the surface of the test cell. *I-V* curves were measured using a computer-controlled digital source meter (Keithley 2440). The area of the solar cells is  $0.196 \text{ cm}^2$ .

### 3. Results and discussion

The XRD pattern of the precipitate from the autoclave reactions was shown in Fig.

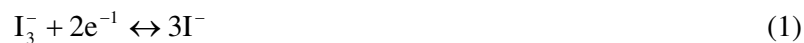
1. All the observed diffraction peaks could be perfectly indexed to the hexagonal system with the lattice constants  $a = 3.615 \text{ \AA}$ ,  $c = 5.283 \text{ \AA}$ , which matched well with the standard data file of  $\text{Co}_{0.85}\text{Se}$  (JCPDS file No. 52-1008). The three strongest peaks of the pattern, at  $2\theta = 33.3^\circ$ ,  $44.9^\circ$  and  $51.1^\circ$ , are assigned to the (101), (102) and (110) planes of the hexagonal close - packed (hcp)  $\text{Co}_{0.85}\text{Se}$ .

SEM was used to study the surface microstructure and morphology of the grown cobalt selenide nanomaterials. Figure 2 shows SEM images of  $\text{Co}_{0.85}\text{Se}$  nanomaterials grown in-situ on the pristine (a, b, c) and the plasma - treated (d, e, f) FTO substrates, and Pt (g, h) on the pristine FTO substrate.  $\text{Co}_{0.85}\text{Se}$  has significantly different surface features on the pristine and the plasma – treated FTO substrates. But, they are composed of widely divided cobalt selenide nanosheets or aggregates. Without plasma treatment,  $\text{Co}_{0.85}\text{Se}$  tended to grow in two dimensions (2D) and extended parallel to the FTO surface, and formed flat nanosheets which are mono dispersive. The typical lateral dimensions of the formed  $\text{Co}_{0.85}\text{Se}$  nanosheets is between 100 nm - 300 nm shown in Figs. 2 (a)-(c). In contrast, with the assistance of the plasma-treatment,  $\text{Co}_{0.85}\text{Se}$  grew in 3D dimensions, considerably developed both parallel and perpendicular to the FTO surface, and formed tremelliform nanosheets with much larger lateral dimensions of 300 nm -1500 nm, as shown in Figs. 2 (d) - (f). Many  $\text{Co}_{0.85}\text{Se}$  tremelliform nanocrystals clustered together on the FTO, clearly shown in Fig. 2 (d). Figures 2 (g) and (h) show typical SEM images of the platinum film of the electrode prepared by thermal decomposition. The formed Pt particles (1–5 nm in size) were unevenly distributed. Similar to the situation of  $\text{Co}_{0.85}\text{Se}$  nanomaterials grown in-situ on the plasma - treated FTO substrates (Fig. 2 (d)), some platinum particles aggregated to form large clusters of about 1-2  $\mu\text{m}$  in size on the  $\text{SnO}_2$  particles of the FTO substrate, as shown as in Figs. 2 (g) and (h). Nevertheless, Pt has much smaller grain size and much higher grain density than  $\text{Co}_{0.85}\text{Se}$  grown on either the pristine or the plasma – treated FTO substrates in Fig. 2 (c), (f) and (h).

From the SEM measurement results in the above, the formed flat  $\text{Co}_{0.85}\text{Se}$  on the pristine FTO shown in Figs. 2 (a) - (c) is analogue to the curled leaf or graphene like  $\text{Co}_{0.85}\text{Se}$  which was grown by the same chemical system as ours but with a longer time (12 h) [16]. Due to reduction or elimination of surface contamination, the plasma treatment improved the wettability of the FTO substrate and enhanced its surface energy [33], increasing the growth rate, the grain size and specific area of the  $\text{Co}_{0.85}\text{Se}$  nanomaterial. Tremelliform  $\text{Co}_{0.85}\text{Se}$  nanosheets with larger accessible surface areas were successfully in-situ synthesized on the plasma – treated FTO substrate as shown in Figs. 2 (d) - (f). This result is consisted with that reported by Liu et al [34]. In their work, tremelliform  $\text{Co}_{0.85}\text{Se}$  sheet powders were fabricated through a autoclave chemical reaction of  $\text{Co}(\text{NO}_3)_2 \cdot 6\text{H}_2\text{O}$ ,  $\text{Na}_2\text{SeO}_3$  and  $\text{N}_2\text{H}_4 \cdot \text{H}_2\text{O}$  at 140 °C for 24 h. Our tremelliform like  $\text{Co}_{0.85}\text{Se}$  nanosheets, by contrast, were obtained at lower temperature and shorter time. Compared to the case without plasma treatment, the size and loading of  $\text{Co}_{0.85}\text{Se}$  obviously increases on the FTO substrate, which can enhance the surface area and active catalytic sites in the CE material. Actually, Liu et al have characterized the specific surface areas of the as-deposited  $\text{Co}_{0.85}\text{Se}$  tremelliform nanosheet powders by the Brunauer – Emmer - Teller (BET) method [34]. They found that the tremelliform  $\text{Co}_{0.85}\text{Se}$  had specific surface area of  $55.1 \text{ m}^2 \text{ g}^{-1}$ , and this value was much higher than those of graphene-like  $\text{Co}_{0.85}\text{Se}$  nanocrystallines ( $11.8 \text{ m}^2 \text{ g}^{-1}$ ) and Pt nanoparticles ( $5.8 \text{ m}^2 \text{ g}^{-1}$ ) reported by Gong et al [16]. From SEM images in Figures 2 a- c of our paper and Figures 3 a and b of ref. 16,

the surface area of Co<sub>0.85</sub>Se flat nanosheets grown without plasma treatment in our work is smaller than that (11.8 m<sup>2</sup> g<sup>-1</sup>) in the latter. The formed Co<sub>0.85</sub>Se tremelliform nanosheets on the plasma - treated FTO possess a much larger specific area, which can be expected to form considerably larger contact surface area between the CE and electrolyte and speed up the diffusion of the electrolyte, thus in turn improving the electrocatalytic activity in the DSSCs. This effect was proved by the subsequent electrochemical and photovoltaic measurements. Therefore, plasma treatment of FTO glass prior to the deposition of cobalt selenide improved the morphological property and the quality of the deposited cobalt selenide CE.

CV experiments were carried out to characterize the electrocatalytic activity of Pt and in-situ grown Co<sub>0.85</sub>Se CEs toward triiodide reduction in an I<sup>-</sup> / I<sub>3</sub><sup>-</sup> redox solution. The Co<sub>0.85</sub>Se CEs with or without plasma treatment behave quite similarly to the Pt/FTO electrode and exhibit two distinct pairs of oxidation and reduction peaks [35]. The relative negative or left pair is assigned to the redox reaction (1) and the positive one is assigned to redox reaction (2) [36].



Cobalt selenides show similar cathodic and anodic peaks compared to Pt, indicating that these selenides are effective in catalyzing the reduction of triiodide to iodide. The characteristics of the left pair peaks are at the focus of our analysis because the CE is responsible for catalyzing the reduction of I<sub>3</sub><sup>-</sup> to I<sup>-</sup> in a DSSC. Thus, the magnitude

of current density at the left reduction peak ( $I_p$ ) is directly proportional to the ability of the electrode to reduce the  $I_3^-$  species. From the bottom left corner of CV images shown in Fig. 3, the absolute  $I_p$  value of the  $Co_{0.85}Se$  CE with DC plasma treatment was  $2.03 \text{ mA cm}^{-2}$  which was significantly higher than that of  $Co_{0.85}Se$  sample without plasma treatment ( $1.04 \text{ mA cm}^{-2}$ ), demonstrating higher catalyst activity towards  $I^-/I_3^-$  redox reaction and faster reaction rate. These could be attributed to the unique physical structure of the former sample shown in Fig. 2. Compared to the case without plasma treatment, the size and loading of  $Co_{0.85}Se$  obviously increases on the FTO substrate, enhancing the surface area and active catalytic sites in the CE material. Moreover, the formed 3D cobalt selenide tremelliform network can allow the rapid diffusion of  $I_3^-$  to access the active sites and subjects to catalytic reduction toward  $I^-$ , therefore improving the electrocatalytic activity in the solar cell. The absolute  $I_p$  value of the Pt CE is  $0.98 \text{ mA cm}^{-2}$ . The first and second highest peak current densities of  $Co_{0.85}Se$  CE with or without DC plasma pre-treatment, respectively, reveal that  $Co_{0.85}Se$  is a remarkable electrochemical catalyst for the reduction of  $I_3^-$ .

To further evaluate the electrocatalytic activity of the as-prepared CEs for the reduction of triiodide, EIS tests were performed, as shown in Figure 4. The corresponding resistances were fitted with Nova software (v1.9, Metrohm Autolab) in terms of the equivalent circuit shown in the inset of Fig. 4. Generally, the typical Nyquist plots of the DSSC shows three semicircles in the measured frequency from 0.1 Hz to 100 kHz. The Ohmic serial resistance ( $R_s$ ) is associated with the series

resistance of the electrolytes and electric contacts in the DSSCs.  $R_{ct1}$ ,  $R_{ct2}$  and  $R_{ct3}$  correspond to the charge transfer processes occurring at the counter electrode (corresponding to the first arc), the  $\text{TiO}_2/\text{dye}/\text{electrolyte}$  interface (corresponding to the second arc) and the Warburg diffusion process of  $\text{I}^-/\text{I}_3^-$  in the electrolyte (corresponding to the third arc), respectively [31, 32]. The  $R_s$  values of the  $\text{Co}_{0.85}\text{Se}$ -based DSSCs on the pristine and the plasma-treated FTO slides are  $18.79 \Omega \text{ cm}^2$  and  $17.61 \Omega \text{ cm}^2$ , respectively. Both values are higher than the  $R_s$  ( $11.9 \Omega \text{ cm}^2$ ) of the DSSC fabricated using the Pt CE. Considering that  $\text{Co}_{0.85}\text{Se}$  and Pt based DSSCs were made by the same types of electrolyte and FTO substrate, the higher  $R_s$  can be attributed to the lower conductivity of  $\text{Co}_{0.85}\text{Se}$  than the metal Pt. However, compared to the case of the device based on the Pt CE, the charge transfer resistance ( $R_{ct1}$ ) at the counter electrode was dramatically decreased when  $\text{Co}_{0.85}\text{Se}$  CEs with plasma pre-treatment were used. The  $R_{ct1}$  of the DSSC with  $\text{Co}_{0.85}\text{Se}$  CE on the plasma-treated FTO was only  $7.05 \Omega \text{ cm}^2$ . This value was much smaller than that ( $14.88 \Omega \text{ cm}^2$ ) of Pt-based DSSC, and also smaller than that ( $12.49 \Omega \text{ cm}^2$ ) of the cell based on the  $\text{Co}_{0.85}\text{Se}$  CE without plasma treatment, suggesting that the  $\text{Co}_{0.85}\text{Se}$  CE with plasma treatment had the best electrocatalytic activity for  $\text{I}_3^-$  reduction.

Figure 5 shows photocurrent density voltage ( $J$ - $V$ ) curves of DSSCs fabricated with two kinds of  $\text{Co}_{0.85}\text{Se}$  CEs and Pt electrode, respectively, under a light intensity of  $100 \text{ mW cm}^{-2}$ . The average measured diode parameters for these cells based on different electrodes along with statistics are summarized in Table I. The

photovoltaic parameters including short circuit current density ( $J_{sc}$ ), open circuit voltage ( $V_{oc}$ ), power conversion efficiency ( $\eta$ ) and fill factor ( $FF$ ) are listed in the table. The DSSC based on the Pt CE showed a  $J_{sc}$  of  $16.79 \text{ mA cm}^{-2}$ , a  $V_{oc}$  of  $0.72 \text{ V}$  and a  $FF$  of  $63.36\%$ , therefore an overall  $\eta$  of  $7.66\%$ . The DSSC fabricated with  $\text{Co}_{0.85}\text{Se}$  CE with or without plasma treatment showed enhanced  $FF$  values of  $67.78\%$  and  $67.03\%$ , respectively. The DSSC with  $\text{Co}_{0.85}\text{Se}$  CE on the plasma-treated FTO showed a  $J_{sc}$  value of  $16.25 \text{ mA cm}^{-2}$  and  $FF$  value of  $67.78\%$ , and thus, the highest  $\eta$  value of  $8.04\%$ , which is conspicuously higher than that ( $7.66\%$ ) for the DSSC with the Pt CE, and also superior to that of the device with  $\text{Co}_{0.85}\text{Se}$  CE on the pristine FTO.

Previous studies have demonstrated that, a counter-electrode usually affects the performance of cell in three aspects: the first is the electrical property or sheet resistance; the second is the electrochemical property or catalysis efficiency, which is determined typically by the inverse of charge transfer resistance; and the last the optical property or reflection of illumination [6, 37-40]. The redox reaction resistance  $R_{ct1}$  at the counter-electrode, the resistance  $R_{ct3}$  of carrier transport by ions in the electrolyte and resistance  $R_s$  due to the sheet resistance of TCO contribute to the internal series resistance of the cell [39]. These resistances bring negative effect on the fill factor and thus, the energy conversion efficiency. The DSSC based on  $\text{Co}_{0.85}\text{Se}$  CE with DC plasma - treatment showed the lowest resistance  $R_{ct1}$ . In view of the fact that  $\text{Co}_{0.85}\text{Se}$  and Pt based DSSCs were made by the same types of electrolyte,  $\text{TiO}_2$

photoanode and FTO substrate, the lowest value of  $R_{ct1}$  led to the lowest internal series resistance, and resulted in the highest fill factor and the highest energy conversion efficiency of the device shown in Fig. 5 and Table 1. The first and second lowest value of  $R_{ct1}$  for the DSSCs based on the two  $\text{Co}_{0.85}\text{Se}$  CEs also indicated that the electrochemical property or catalysis efficiency of  $\text{Co}_{0.85}\text{Se}$  CE is better than that of Pt. The conclusions of the catalytic activity and the photovoltaic performance derived from the CV, EIS and  $J$ - $V$  data for the cobalt selenide and Pt CEs are consistent.

#### 4. Conclusions

We have investigated plasma treatment of FTO glass for improving the performance of cobalt selenide CE for DSSCs. The FTO glass substrates were treated using  $\text{O}_2/\text{Ar}$  DC plasma prior to the cobalt selenide growth. The surface morphology of cobalt selenide in-situ synthesized on the plasma modified FTO substrate changed dramatically compared to the case without plasma modification. EIS, CV and  $J$ - $V$  measurements show consistent results, which can be associated with the unique physical structures of the  $\text{Co}_{0.85}\text{Se}$  CEs. With plasma treatment, the size and loading of  $\text{Co}_{0.85}\text{Se}$  was obviously increased, and tremelliform  $\text{Co}_{0.85}\text{Se}$  nanosheets were formed on the FTO substrate. This  $\text{Co}_{0.85}\text{Se}$  CE has enhanced active catalytic sites, a larger accessible surface area and better catalytic properties. The charge transfer resistance ( $R_{ct1}$ ) at the counter electrode is considerably decreased when  $\text{Co}_{0.85}\text{Se}$  CEs with plasma treatment is used, compared to the case of the Pt or the  $\text{Co}_{0.85}\text{Se}$  CEs

without plasma treatment. The cell with the  $\text{Co}_{0.85}\text{Se}$  on the plasma-treated FTO produces an energy conversion efficiency of 8.04%. This photovoltaic performance is conspicuously better than that for the DSSC with the Pt CE (7.66%), and also superior to that (7.88%) for the device with the  $\text{Co}_{0.85}\text{Se}$  CE on the pristine FTO without plasma treatment.

### **Acknowledgement**

This work was supported by National Natural Science Foundation of China (Nos. 11274119, 61275038) and Large Instruments Open Foundation of East China Normal University.

## References

- [1] B. O'Regan and M. Grätzel, *Nature*, 1991, 353, 737-724.
- [2] A. Kay, M. Grätzel, *Sol. Energy Mater. Sol. Cells*, 1996, 44, 99-117.
- [3] S. Mathew, A. Yella A, P. Gao, R. Humphry-Baker, B. F. Curchod and N. Ashari-Astani, *Nat. Chem.*, 2014, 6, 242-247.
- [4] M. Grätzel, *J. Photochem. Photobiol. A: Chem.*, 2004, 164, 3-14.
- [5] S. Ahmad, J. H. Yum, Z. Xianxi, M. Grätzel, H. J. Butt and M. K. Nazeeruddin M K, *J. Mater. Chem.*, 2010, 20, 1654-1658.
- [6] D. Zhang, X. Li, H. Li, S. Chen, Z. Sun, X. J. Yin and S. M. Huang, *Carbon* 2011, 49, 5382-5388.
- [7] X. H. Miao, K. Pan, Q. J. Pan, W. Zhou, L. Wang, Y. P. Liao, G. H. Tian and G. F. Wang, *Electrochim. Acta*, 2013, 96, 155-163.
- [8] K. Suzuki, M. Yamamoto, M. Kumagai and S. Yanagida, *Chem. Lett.*, 2003, 32, 28-29.
- [9] D. W. Zhang, X. D. Li, S. Chen, F. Tao, Z. Sun, X. J. Yin and S. M. Huang, *J. Solid State Electrochem.*, 2010, 14, 1541-1546.
- [10] Y. P. Liao, K. Pan, L. Wang, Q. J. Pan, W. Zhou, X. H. Miao, B. J. Jiang, C. G. Tian, G. H. Tian, G. F. Wang and H. G. Fu, *ACS Appl. Mater. Interfaces*, 2013, 5, 3663-3670.
- [11] M. X. Wu, X. Lin, Y. D. Wang, L. Wang, W. Guo, D. Qi, X. J. Peng, A. Hagfeldt, M. Gratzel and T. L. Ma, *J. Am. Chem. Soc.*, 2012, 134, 3419-3428.
- [12] Q. W. Jiang, G. R. Li and X. P. Gao, *Chem. Commun.*, 2009, 6720-6722.

- [13] X. Xin, M. He, W. Han, J. Jung and Z. Lin, *Angew. Chem., Int. Ed.*, 2011, 50, 11739-11742.
- [14] H. K. Mulmudi, S. K. Batabyal, M. Rao, R. R. Prabhakar, N. Mathews and Y. M. Lam, *Phys. Chem. Chem. Phys.*, 2011, 13, 19307-19309.
- [15] Z. Li, F. Gong, G. Zhou and Z. S. Wang, *J. Phys. Chem. C*, 2013, 117, 6561-6566.
- [16] F. Gong, H. Wang, X. Xu, G. Zhou and Z. S. Wang, *J. Am. Chem. Soc.*, 2012, 134, 10953-10958.
- [17] J. Shen, D. Zhang, J. Li, X. Li, Z. Sun and S. Huang, *Nano-Micro Lett.*, 2013, 5, 281-288.
- [18] X. Y. Cheng, Z. J. Zhou, Z. L. Hou, W. H. Zhou and S. X. Wu, *Sci. Adv. Mater.*, 2013, 5, 1193-1198.
- [19] Sara Thomas, T. G. Deepak, G. S. Anjusree, T. A. Arun, Shantikumar V. Nair and A. Sreekumaran Nair, *J. Mater. Chem. A*, 2014, 2, 4474-4490.
- [20] F. Gong, X. Xu, Z. Li, G. Zhou and Z. S. Wang, *Chem. Commun.*, 2013, 49, 1437-1439.
- [21] Z. Zhang, S. Pang, H. Xu, Z. Yang, X. Zhang, Z. Liu, X. Wang, X. Zhou, S. Dong and X. Chen, *RSC Adv.*, 2013, 3, 16528-16533.
- [22] J. Guo, Y. Shi, C. Zhu, L. Wang, N. Wang and T. Ma, *J. Mater. Chem. A*, 2013, 1, 11874-11879.
- [23] K. Ostrikov, in *Plasma Nanoscience: Basic Concepts and Applications of Deterministic Nanofabrication*, Wiley-VCH Verlag GmbH & Co. KGaA,

- Weinheim, 2008.
- [24] C. C. Wu, C. I. Wu, J. C. Sturm and A. Kahn, *Appl. Phys. Lett.*, 1997, 70, 1348-1350.
- [25] A. Y. Polyakov, N. B. Smirnov, A. V. Govorkov, K. Ip, M. E. Overberg, Y. W. Heo, D. P. Norton, S. J. Pearton, B. Luo, F. Ren and J. M. Zavada, *J. Appl. Phys.*, 2003, 94, 400-406.
- [26] M. S. Choi, Y. J. Lee, J. D. Kwon, Y. Jeong, J. Y. Park, Y. C. Ang, P. K. Song, and D. H. Kim, *Curr. Appl. Phys.*, 2013, 13, 1589-1593.
- [27] X. Zhang, M. Jin, Z. Liu, D. A. Tryk, S. Nishimoto, T. Murakami and A. Fujishima, *J. Phys. Chem. C*, 2007, 111, 14521-14529.
- [28] Y. S. Kim, B. J. Yoo, R. Vittal, Y. Lee, N. G. Park and K. J. Kim, *J. Power Sources*, 2008, 175, 914-919.
- [29] M. Konstantakou, T. Stergiopoulos, V. Likodimos, G. C. Vougioukalakis, L. Sygellou, A. G. Kontos, A. Tserepi and P. Falaras, *J. Phys. Chem. C*, 2014, DOI: 10.1021/jp412766f
- [30] N. Pappas, M. Grätzel, Process for manufacturing an electrode for an electrochemical device, Polytechnique Federale Lausanne DE EP0852804, 1999.
- [31] Y. H. Lai, C. Y. Lin, J. G. Chen, C. C. Wang, K. C. Huang, K. Y. Liu, K. F. Lin, J. J. Lin and K. C. Ho, *Sol. Energy Mater. Sol. Cells*, 2010, 94, 668-674.
- [32] G. Zhu G, X. J. Wang X J, H. L. Li H L, L. K. Pan L K, H. C. Sun H C, X. J. Liu, T. Lv and Z. Sun, *Chem. Commun.*, 2012, 48, 958-960.
- [33] F. Lisco, A. Abbas, B. Maniscalco, P. M. Kaminski, M. Losurdo, K. Bass, G.

- Claudio and J. M. Walls, *J. Renewable Sustainable Energy*, 2014, 6, 011202.
- [34] C. C. Liu, J. M. Song, J. F. Zhao, H. J. Li, H. S. Qian, H. L. Niu, C. J. Mao, S. Y. Zhang and Y. H. Shen, *Appl. Catal. B: Environ.*, 2012, 119-120, 139-145.
- [35] Z. Huang, X. Liu, K. Li, D. Li, Y. Luo, H. Li, W. Song, L. Chen and Q. Meng, *Electrochem. Commun.*, 2007, 9, 596-598.
- [36] M. Wu, X. Lin, A. Hagfeldt and T. Ma, *Chem. Commun.*, 2011, 47, 4535-4537.
- [37] A. Hauch and A. Georg, *Electrochim Acta*, 2001, 46, 3457-3466.
- [38] Q. Wang, J. E. Moser and M. Grätzel, *J. Phys. Chem. B*, 2005, 109 , 14945-14953.
- [39] L. Han, N. Koide, Y. Chiba and T. Mitate, *Appl. Phys. Lett.*, 2004, 84, 2433-2435.
- [40] L. Han, N. Koide, Y. Chiba, A. Islam, R. Komiya, N. Fuke, A. Fukui and R. Yamanaka, *Appl. Phys. Lett.*, 2005, 86, 213501.

**Figure captions**

Figure 1 XRD pattern of the obtained  $\text{Co}_{0.85}\text{Se}$  powders

Figure 2 SEM images of  $\text{Co}_{0.85}\text{Se}$  in-situ grown on the pristine (a, b, c) and the plasma - treated (d, e, f) FTO substrates, and Pt (g, h) on the pristine FTO substrate

Figure 3 CV curves of the Pt electrode and  $\text{Co}_{0.85}\text{Se}$  CEs with and without DC plasma treatment. The scan rate and scan voltage range are  $50 \text{ mV s}^{-1}$  and  $-0.4 \sim 1.0 \text{ V}$ , respectively

Figure 4 Nyquist plots of DSSCs assembled on the Pt electrode and  $\text{Co}_{0.85}\text{Se}$  CEs with and without DC plasma treatment

Figure 5  $J$ - $V$  curves of DSSCs assembled on the Pt electrode and  $\text{Co}_{0.85}\text{Se}$  CEs with and without DC plasma treatment

Table 1 Photovoltaic performance parameters for different CEs

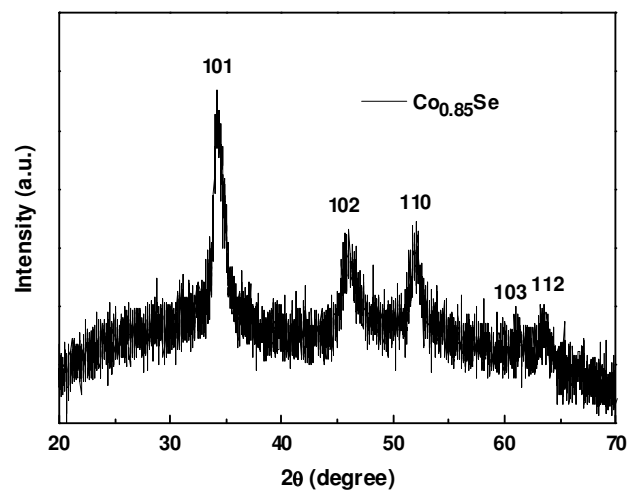
**Fig. 1**

Fig. 2

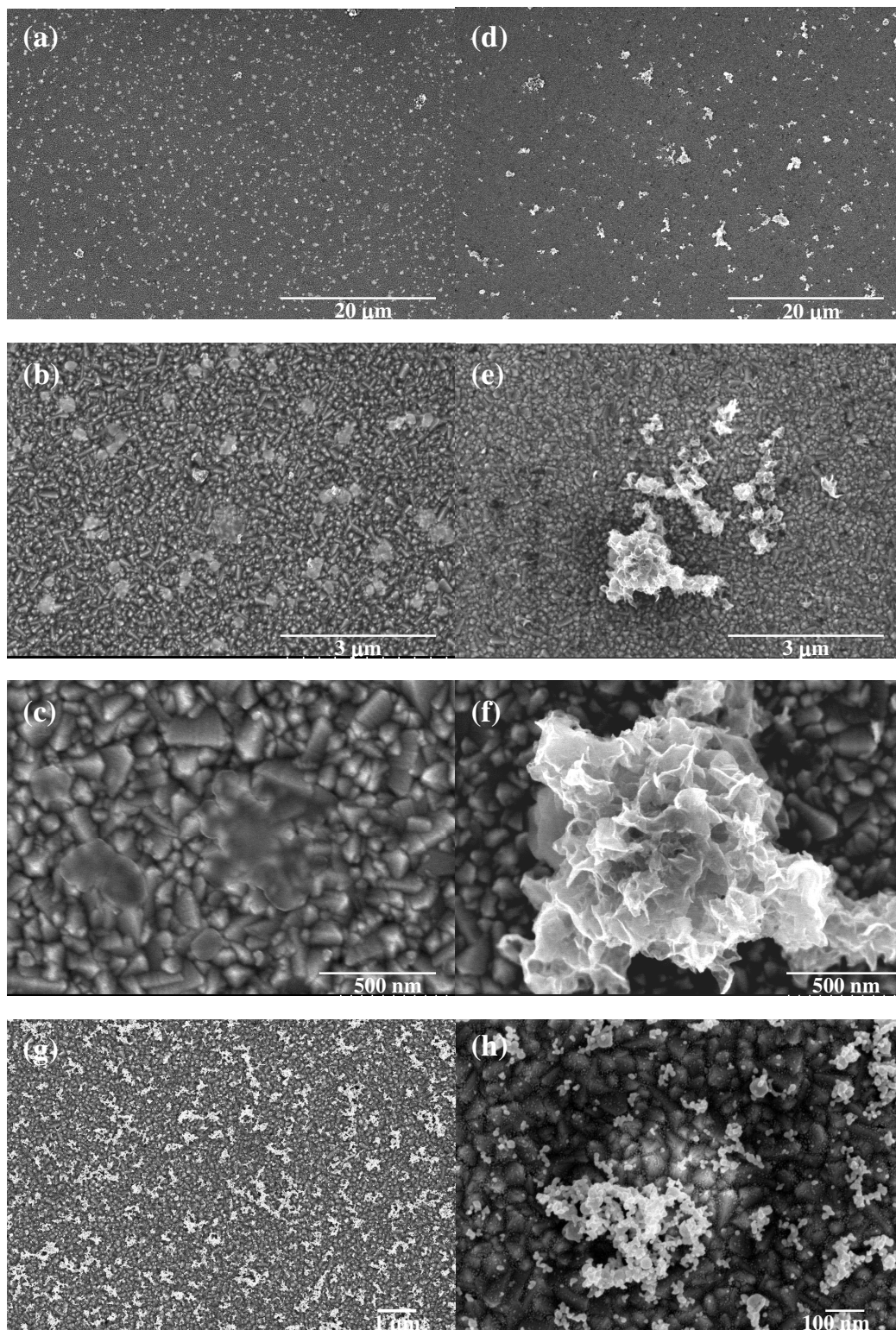


Fig. 3

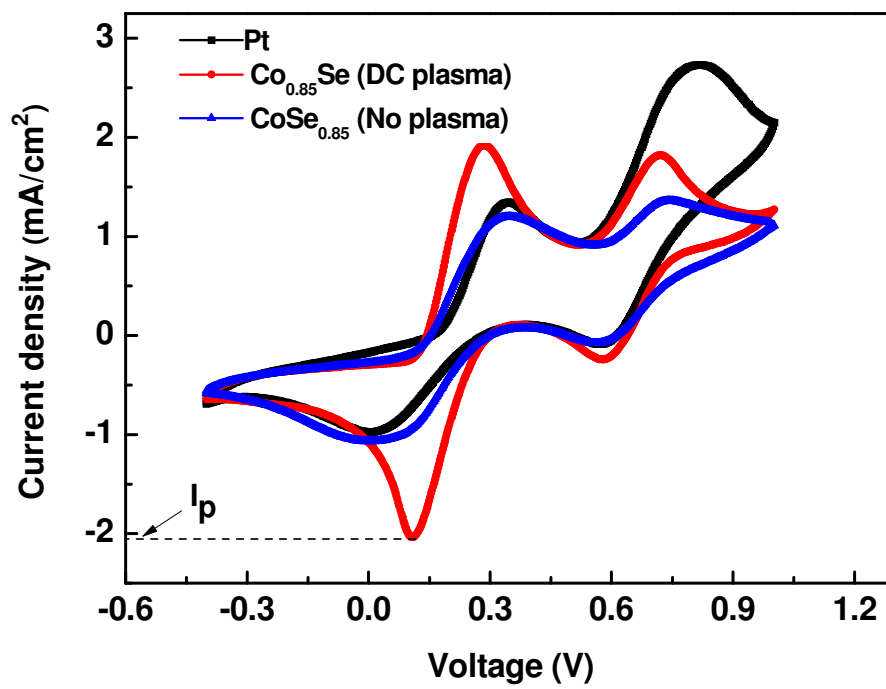


Fig. 4

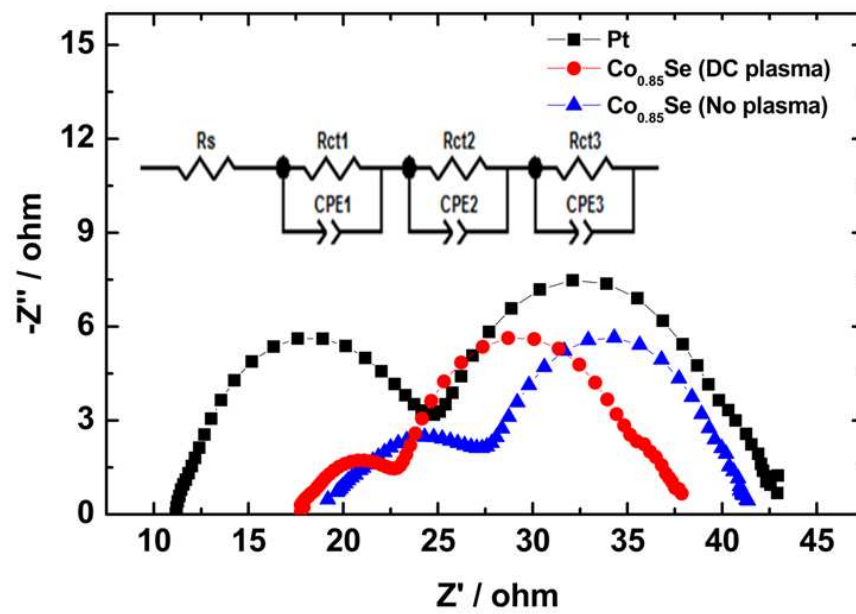
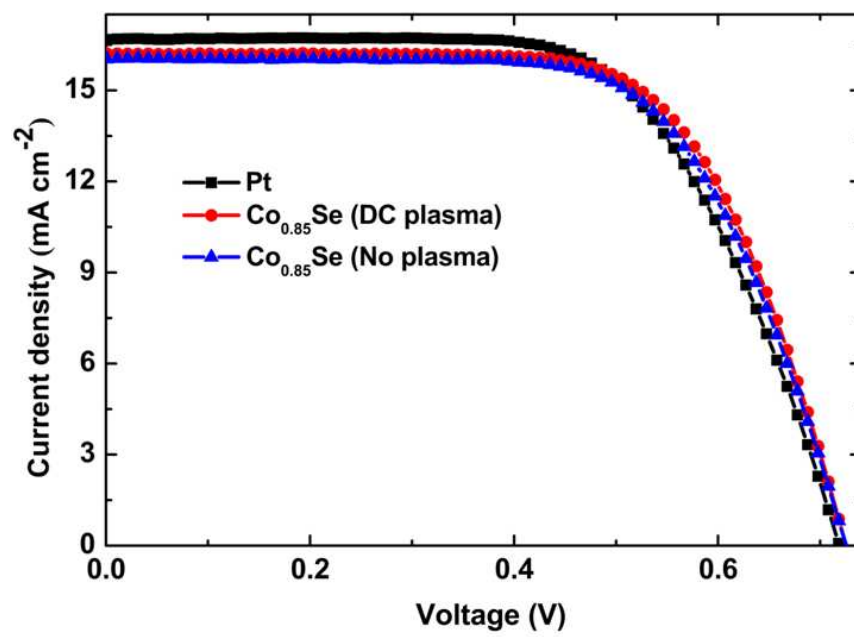


Fig. 5



**Table 1**

CE	$V_{oc}$ (V)	$J_{sc}$ (mA cm <sup>-2</sup> )	FF (%)	$\eta$ (%)
Pt	0.72±0.01	16.79±0.28	63.36±0.01	7.66±0.23
Co <sub>0.85</sub> Se (No plasma)	0.73±0.01	16.10±0.31	67.03±0.02	7.88±0.26
Co <sub>0.85</sub> Se (DC plasma)	0.73±0.01	16.25±0.34	67.78±0.02	8.04±0.28

**for the Table of contents entry**

DC plasma shortened the growth time, improved morphological and electrocatalytic properties of  $\text{Co}_{0.85}\text{Se}$  electrodes, and boosted the efficiency of DSSCs.

